

On the transport properties of microcrystalline silicon

A. Fejfar^{a,*}, N. Beck^b, H. Stuchlíková^a, N. Wyrsh^b, P. Torres^b, J. Meier^b,
A. Shah^b, J. Kočka^a

^a *Institute of Physics, Academy of Sciences of the Czech Republic, Cukrovarnická 10, 162 00 Prague 6, Czech Republic*

^b *Institut de Microtechnique, University of Neuchatel, Rue A.L. Breguet 2, 2000 Neuchatel, Switzerland*

Abstract

To determine the charge collection mechanism in hydrogenated microcrystalline silicon ($\mu\text{c-Si:H}$) solar cells, we have measured the electronic transport properties of $\mu\text{c-Si:H}$ by time-of-flight and by ac capacitance and conductance on a unique $5.6\ \mu\text{m}$ thick sample. We found the electron drift mobility $\mu_{\text{D}} = 2.8 \pm 0.2\ \text{cm}^2\ \text{V}^{-1}\ \text{s}^{-1}$, thermally activated with $E_{\text{A}} = 0.14 \pm 0.1\ \text{eV}$. Evidence for field inhomogeneity was observed as an initial maximum of the photocurrent transients and as an increase of capacitance over the geometrical value. The frequency dependence of the capacitance exhibits marked differences from a-Si:H and is proposed as a tool for studying the effects of microstructure on electronic properties. Changes of the sample capacitance with temperature and illumination were observed. As a consequence of the inhomogeneity of the material, several different activation energies were found: $0.14\ \text{eV}$ for electron drift mobility, $0.29\ \text{eV}$ for ac conductivity, $0.4\ \text{eV}$ for steady state dark conductivity and finally $\geq 0.8\ \text{eV}$ for the photocapacitance relaxation.

Keywords: Microcrystalline silicon; Charge transport; Time-of-flight

1. Introduction

Recently, midgap hydrogenated microcrystalline silicon ($\mu\text{c-Si:H}$) has been successfully used in solar cells with an efficiency of 7.7% (single $\mu\text{c-Si:H}$ p-i-n) [1]. The fully microcrystalline junction is a crucial part of so called ‘micromorph’ tandem (a-Si:H/ $\mu\text{c-Si:H}$) solar cells for which the stabilized efficiency achieved 10.7% [2]. Compared to a-Si:H, higher charge collection in $\mu\text{c-Si:H}$ junctions was observed even for devices with thicknesses in excess

of $3\ \mu\text{m}$ [1] but the mechanism of the carrier collection is not known. The situation is further complicated by the columnar structure of $\mu\text{c-Si:H}$ [3] and thus possible anisotropy of the transport properties. Hall effect, ambipolar diffusion length and photoconductivity measurements performed so far [4,5] measure properties of transport parallel to the substrate whereas for solar cells transport perpendicular to the substrate is crucial. The most promising method is the time-of-flight (TOF) used to study transport in a-Si:H solar cell structures. However, its use for $\mu\text{c-Si:H}$ produced contradictory results [6–8]. The difficulties were related mainly to response time limitations which we explain here as due to thin samples and capacitances larger than geometrical.

* Corresponding author. Fax: +420-2 3123184; e-mail: fejfar@fzu.cz.

On the other hand, it is difficult to obtain thicker samples as these usually peel off due to internal stresses. In this study we report results on a unique $5.6 \mu\text{m}$ thick sample which enabled us to recognize new features in the transients. In addition we report on the difference between the geometrical and experimentally observed capacitance of the samples and we show how the capacitance is changed by illumination and temperature.

2. Experimental results

For the present study, $\mu\text{c-Si:H}$ layers were deposited by very high frequency plasma enhanced chemical vapor deposition described elsewhere [9]. Unless stated otherwise, we report results for the $5.6 \mu\text{m}$ thick $\mu\text{c-Si:H}$ layer deposited by glow discharge at an excitation frequency 130 MHz in silane passed through gas purifier [9] and diluted by hydrogen (5% of silane in total gas flow) on Asahi glass covered by transparent conductive oxide (TCO) type U kept at 220°C . Semitransparent NiCr pads 1 mm in diameter were deposited as top contacts. The other samples included a series of TCO/ $\mu\text{c-Si:H}$ /NiCr samples with thickness around $2.5 \mu\text{m}$ deposited with different discharge powers and a $4.1 \mu\text{m}$ thick n-i-p fully $\mu\text{c-Si:H}$ junction.

Time-of-flight transients were excited by 0.6 ns pulses at $\lambda = 500 \text{ nm}$ (where the absorption coefficient of $\mu\text{c-Si:H}$ is $\alpha \approx 5 \times 10^4 \text{ cm}^{-1}$ [10] and the absorption depth $\approx 0.2 \mu\text{m}$) and recorded on a 50Ω resistor by 500 MHz (2 GS/s) bandwidth oscilloscope. The initial current peak caused oscillations in the measuring circuit which we avoided by numerical low pass filtering which effectively limits the bandwidth to 100 MHz. This value corresponds to the limitation by response time of the circuit which was estimated as $RC = 300 \Omega \times 30 \text{ pF} \approx 10 \text{ ns}$ where the contact resistance 300Ω was estimated from the initial current at full laser illumination when the current is not limited by the sample. The results of the standard small signal TOF measurements on a $5.6 \mu\text{m}$ sample are shown in Figs. 1 and 2.

Ac capacitance and conductance were measured by an impedance analyzer HP 4192A in a frequency range 6 Hz to 13 MHz and the results are shown in Figs. 3–5.

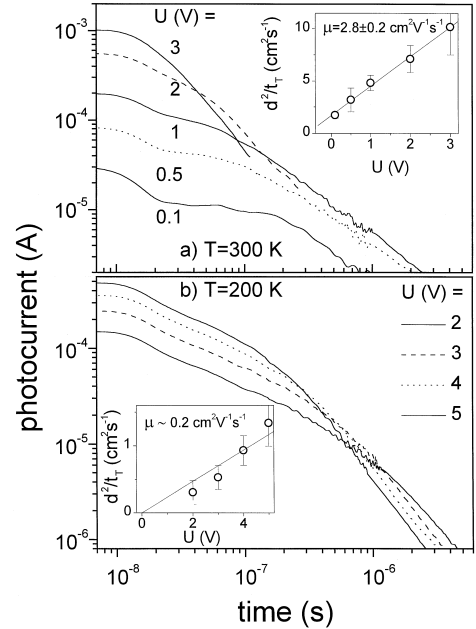


Fig. 1. Time-of-flight electron transients for $5.6 \mu\text{m}$ thick $\mu\text{c-Si:H}$ sample at (a) room temperature and (b) at 200 K and for different applied voltages. The insets show the fits used to obtain mobility.

2.1. Discussion

The results of the standard small signal TOF measurements on a $5.6 \mu\text{m}$ sample are shown in Fig. 1a (room temperature) and Fig. 1b (at 200 K). At

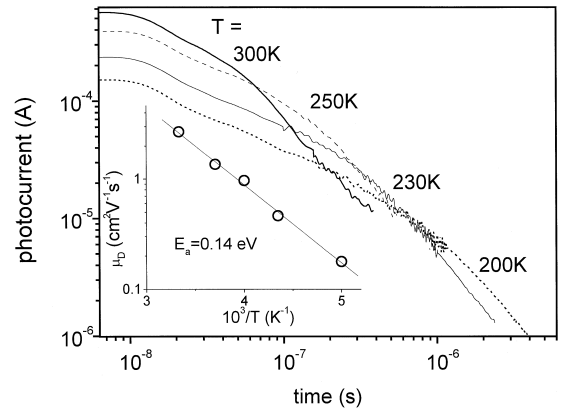


Fig. 2. Temperature dependence of the electron time-of-flight transients at $U_{\text{appl}} = 2 \text{ V}$. The inset illustrates the thermally activated behaviour of the electron mobility together with a fit corresponding to activation energy $E_a = 0.14 \text{ eV}$.

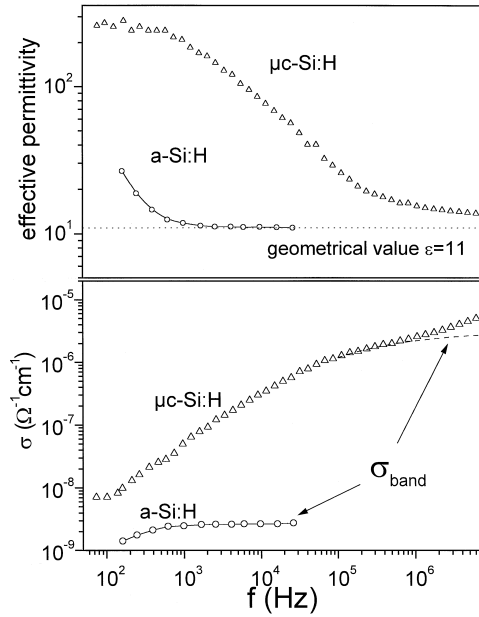


Fig. 3. The frequency dependence of ac conductivity and effective relative permittivity $\epsilon_{\text{eff}} = C \cdot d / (\epsilon_0 \cdot S)$ for the $5.6 \mu\text{m}$ $\mu\text{c-Si:H}$ sample (Δ). The data on a-Si:H (\circ with line to guide eye) are shown for comparison [11]. The arrows mark the plateaus of conductivity where the influence of contacts is minimized.

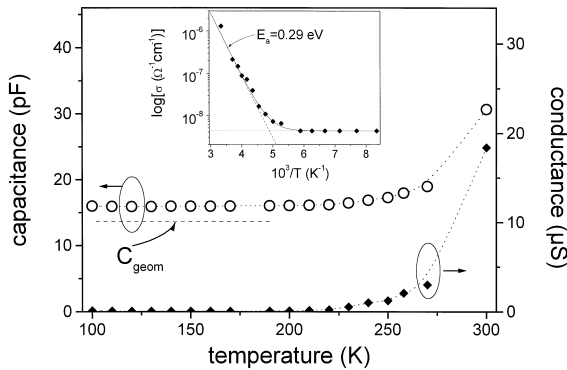


Fig. 4. Temperature dependence of the capacitance (open circles, left axis) and conductance (full diamonds, right axis) of the $5.6 \mu\text{m}$ $\mu\text{c-Si:H}$ sample measured at $f = 100 \text{ kHz}$. Experimental points are connected by dotted lines as a guide to eye. At low temperatures the capacitance approaches the geometrical value (dashed line calculated for $\epsilon_{\text{Si}} = 11$). The increase of capacitance with T seems to be related to the simultaneous increase of the thermally activated conductance (see inset with the conductance data replotted in log scale together with a fit by a sum of exponential with activation energy 0.29 eV and temperature-independent conductivity).

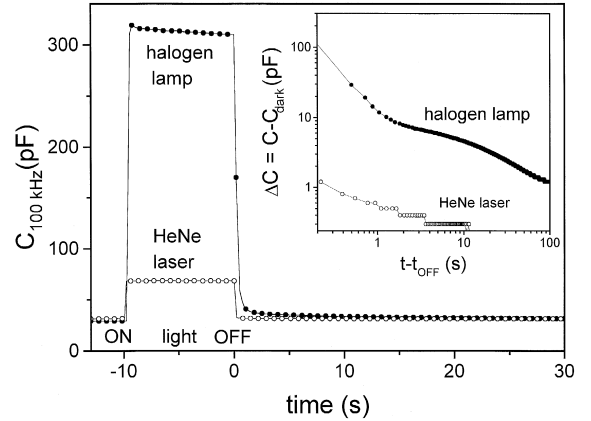


Fig. 5. Increase of the capacitance due to illumination by light of halogen lamp (\bullet) or HeNe laser (\circ) measured on $5.6 \mu\text{m}$ $\mu\text{c-Si:H}$ sample (lines are included as guide to eye). An inset shows that after the light is switched off the capacitance relaxes to the dark value with characteristic time on the order of seconds.

room temperature (Fig. 1a) and at small applied voltage the photocurrent decreases after the initial maximum to a plateau which we assume to be due to the real transit of the electrons to the opposite electrode. At higher voltages the transit becomes so short that it merges with the initial current peak. Even so the fit of d^2/t_T vs. applied voltage, U , was possible (see top part of the inset) and the deduced electron mobility is $2.8 \pm 0.2 \text{ cm}^2 \text{ V}^{-1} \text{ s}^{-1}$.

The transients recorded at 200 K (Fig. 1b) show that the initial current peak is still present even though less pronounced than at room temperature. The photocurrent, following a power law, shows that the electron transport becomes dispersive. Mobility of the electrons at this temperature was $\sim 0.2 \text{ cm}^2 \text{ V}^{-1} \text{ s}^{-1}$.

The temperature dependence of the mobility can be found from Fig. 2 showing the transits at 2 V for different temperatures. An Arrhenius plot shows that the electron drift mobility is thermally activated with the activation energy $0.14 \pm 0.1 \text{ eV}$.

What is the origin of the initial current drop which we usually do not observe on device grade a-Si:H? The drop could be due to extraction of holes to the illuminated contact, capture of the electrons into traps, or to an inhomogeneous electric field near or in the region of the charge photogeneration.

To gain insight into this problem we measured the frequency dependence of ac conductivity and capaci-

tance. The results are shown in Fig. 3 and compared with typical data for a-Si:H [11]. Note the special plot of capacitance in a form of effective relative permittivity $\epsilon_{\text{eff}} = C \cdot d / \epsilon_0 S$ where C is the observed capacitance, d and S are the sample thickness and area, respectively, and ϵ_0 is the vacuum permittivity. If the sample capacitance approaches the geometrical value ϵ_{eff} should be about 11, typical for Si regardless of its structure.

A difference between $\mu\text{c-Si:H}$ and a-Si:H is evident from Fig. 3. For $\mu\text{c-Si:H}$ the measured capacitance exceeds the geometrical value ($\epsilon_{\text{eff}} > 11$) even at 1 MHz. This excess indicates charge accumulation inside the sample and concentration of the field to a fraction of the sample thickness. The field concentration would explain the high capacitance values and also the photocurrent decrease in TOF experiment (Fig. 1) as due to the slow-down of the carriers after they traverse the higher field regions and move into regions of lower electric field.

We believe that the higher field regions are related to ‘grain boundaries’ between crystalline grains. Therefore the frequency dependence of the capacitance (or ϵ_{eff}) should allow us to get information, e.g., about the size distribution of crystallites in $\mu\text{c-Si:H}$. Moreover, the study of ac conductivity also offers us a possibility to separate different transport mechanisms and/or contact effects. At medium frequencies the ‘true’ bulk (band-like) conductivity, σ_{band} [11], free from contact effects, can be deduced. At higher frequencies (see Fig. 3) and/or lower temperatures (Fig. 4, see below) we may observe the evidence of hopping conductivity almost independent of temperature and increasing with frequency ($\approx f^1$).

We have observed that the capacitance of the $\mu\text{c-Si:H}$ samples changes with temperature and bias voltage. The temperature dependencies of the capacitance and conductance measured at 100 kHz on the 5.6 μm sample are shown in Fig. 4. The fit of an Arrhenius function to the conductivity indicates two different mechanisms of conductivity: thermally activated ‘band-like’ with $E_a \approx 0.29$ eV and a temperature independent hopping $\sigma_{100 \text{ kHz}} \approx 5 \cdot 10^{-9} \Omega^{-1} \text{cm}^{-1}$.

Even larger changes of the capacitance may be observed under illumination. When illuminated by halogen lamp (roughly corresponding to standard

AM1 illumination) the $\mu\text{c-Si:H}$ sample capacitance increases more than 10 times (see Fig. 5) while for a-Si:H the change is negligible. This change would correspond to shrinkage of the higher field regions. After the light is switched off the capacitance relaxes back to its dark value. The plot of the photocapacitance $\Delta C(t) = C(t) - C_{\text{dark}}$ shows that the relaxation process has a time constant on the order of several seconds. The magnitude of $\Delta C(t)$ depends on the light intensity. The underlying mechanisms of this relaxation is not known. We may only hypothesize that it is due to the carriers trapped in the deep states when the higher field region shrinks and which have to wait until they are thermally emitted after the high field region expands to its dark value again. Therefore the underlying physical mechanism would be similar to post-transit photocurrent [12]. If we used the attempt-to-escape frequency $\nu_0 = 10^{13}$ Hz typical for a-Si:H the depth of traps corresponding to the time ≈ 1 s would be ≈ 0.8 eV. So deep states can hardly be expected in the crystalline Si grains with gap 1.1 eV, however, they may exist in the amorphous component or they may be related to the intergrain barriers caused by charges trapped at the boundaries [13,14] or to the band edge discontinuities between amorphous and crystalline components [15].

It is interesting to note that several activation energies were observed in this study: 0.14 eV for electron drift mobility, 0.29 eV for ac conductivity compared to 0.4 eV for steady state dark conductivity and finally ≥ 0.8 eV for ΔC relaxation. This finding corresponds to wide and strong frequency dependence of measured capacitance, probably due to distribution of crystallite sizes.

3. Conclusions

Results of both time-of-flight and capacitance study indicate high field regions in $\mu\text{c-Si:H}$, possibly related to crystallites and their boundaries. Different activation energies for drift mobility, dc and ac conductivity and photocapacitance relaxation show that the material inhomogeneity leads to several possible transport mechanisms. The ac response measurements are suggested as a perspective new tool

for studying $\mu\text{-c-Si:H}$ which could separate different transport mechanisms from the contact effects and characterize the distribution of crystallites.

Acknowledgements

This work was supported by projects JOR3-CT97-0145, A1010528 and GAČR 202/95/1445.

References

- [1] J. Meier, P. Torres, R. Platz, S. Dubail, U. Kroll, J.A. Anna Selvan, N. Pellaton Vaucher, Ch. Hof, D. Fischer, H. Keppner, A. Shah, K.-D. Ufert, P. Giannoulés, J. Koehler, MRS spring meeting, San Francisco 1996, MRS Proc. 420, 1996, p. 3.
- [2] H. Keppner, P. Torres, J. Meier, R. Platz, D. Fischer, U. Kroll, S. Dubail, J.A. Anna Selvan, N. Pellaton Vaucher, Y. Ziegler, R. Tscharnner, Ch. Hof, N. Beck, M. Goetz, P. Pernet, M. Goerlitzer, N. Wyrsh, J. Veuille, J. Cuperus, A. Shah, J. Pohl, MRS Proc. 452 (1996) 427.
- [3] J. Meier, S. Dubail, R. Flückiger, D. Fischer, H. Keppner, A. Shah, Proc. of the 1st WCPVEC, HI, 1994, p. 405.
- [4] P.G. LeComber, G. Willeke, W.E. Spear, J. Non-Cryst. Solids 59–60 (1983) 795.
- [5] M. Goerlitzer, N. Beck, P. Torres, J. Meier, N. Wyrsh, J. Appl. Phys. 80 (1996) 5111.
- [6] N. Wyrsh, M. Goerlitzer, N. Beck, J. Meier, A. Shah, MRS Spring meeting, San Francisco 1996, MRS Proc. 420, 1996, p. 801.
- [7] N. Beck, P. Torres, J. Fric, Z. Remeš, A. Poruba, Ha Stuchlíková, A. Fejfar, N. Wyrsh, M. Vaňeček, J. Kočka, A. Shah, MRS Fall Meeting, Boston, 1996, MRS Proc. Vol. 452, 1997, p. 761.
- [8] N. Beck, PhD thesis, Neuchatel University, 1997.
- [9] P. Torres, J. Meier, R. Flückiger, U. Kroll, J.A. Anna Selvan, H. Keppner, A. Shah, S.D. Littelwood, I.E. Kelly, P. Giannoulés, Appl. Phys. Lett. 69 (1996) 1373.
- [10] N. Beck, J. Meier, J. Fric, Z. Remeš, A. Poruba, R. Flückiger, J. Pohl, A. Shah, M. Vaněček, J. Non-Cryst. Solids 198–200 (1996) 903.
- [11] J. Kočka, M. Vaněček, O. Štika, Q. Dung-Tring, J. Stuchlík, A. Tříška, Proc. 8th EC-PVSEC, Florence, Italy, 1988, Kluwer Acad. Publ., p. 724.
- [12] G.F. Seynhaeve, R.P. Barclay, G.J. Adriaenssens, J.M. Marshall, Phys. Rev. B 39 (14) (1989) 10196.
- [13] J.Y.W. Seto, J. Appl. Phys. 46 (1975) 5247.
- [14] G. Baccarani, B. Ricco, G. Spadini, J. Appl. Phys. 49 (1978) 5565.
- [15] X. Xu, J. Yang, A. Banerjee, S. Guha, K. Vasanth, S. Wagner, Appl. Phys. Lett. 67 (1995) 2323.